DESIGN AND FINITE ELEMENT ANALYSIS OF AN ANKLE JOINT IMPLANT: A COMPARATIVE STUDY OF BIOMATERIALS UNDER PHYSIOLOGICAL LOADING CONDITIONS

[1]Assistant professor, Department of Mechanical Engineering, Sagi Rama Krishnam Raju Engineering College, Bhimavaram-534204, Andhra Pradesh, India
[2]B.Tech Students, Department of Mechanical Engineering, Sagi Rama Krishnam Raju Engineering College, Bhimavaram-534204, Andhra Pradesh, India
[1] N V S Swamy Chinamilli
[2] Santharao Kovviri, [2]Dum Dum Manoj Kumar Nulakani, [2]Venkata Naga Siva Kishore Pasupuleti ,
[2]Manoj Kumar Rapaka, [2]Veera Anjaneyulu Padavala,
[1]swamy.chinamilli@gmail.com

ABSTRACT

The design and structural analysis of an ankle joint implant were carried out using CATIA for modeling and ANSYS for finite element analysis, focusing on static and modal behavior under physiological loads of 2500 N and 3500 N. A comparative evaluation of implant materials—CoCrMo, Ti-6Al-7Nb, Ti-13Nb-13Zr, and SS 316—was performed to assess von Mises stress, shear stress, deformation, and natural frequencies. Results indicate a linear increase in von Mises and shear stresses with increasing load for all materials. However, CoCrMo consistently demonstrated the lowest von Mises stress (71.581–90.927 MPa), lowest shear stress (41.328–52.483 MPa), minimal deformation (0.161 mm), and the highest natural frequencies, reflecting superior stiffness and vibration resistance. Titanium alloys exhibited moderate mechanical performance, while SS 316 showed significantly higher deformation (up to 3.642 mm) and reduced structural stability. The findings confirm that CoCrMo offers exceptional mechanical stability, stress resistance, and durability, making it the most suitable material for ankle joint implants subjected to high biomechanical loads and demanding physiological conditions.

1 INTRODUCTION

1.1 INTRODUCTION

Recent studies have extensively investigated the design and biomechanical performance of ankle joint prostheses using computational and experimental approaches. Nazha et al. (2024) evaluated the biomechanical behavior of artificial ankle joints through finite element analysis by comparing titanium alloys, cobalt–chromium–molybdenum alloys, and UHMWPE, concluding that material selection significantly influences stress distribution and deformation under physiological loading conditions. Akhmejanov et al. (2025) designed and analyzed a two-degree-of-freedom autonomous active ankle–foot prosthesis using CAD modeling and finite element techniques, demonstrating improved mobility, load-bearing capacity, and dynamic gait performance. Lee and Lee (2025) proposed a novel methodology for determining optimal component sizing in total ankle replacement systems, which enhanced implant alignment and reduced stress concentrations within ankle joint components. Hassan et al. (2026) developed a porous total ankle arthroplasty implant to promote bone in-growth and reduce micromotion, with finite element simulations confirming superior biomechanical stability compared to conventional solid implants. Li et al. (2024) introduced a bio-inspired intelligent ankle–foot prosthesis based on human anatomical structure and motion bionics, achieving improved adaptability and functional performance during walking cycles. Pace et al. (2025) presented a cam-driven hydraulic prosthetic ankle and optimized its design through simulation-based methods, highlighting enhanced energy recovery and smoother ankle motion during gait. Zhou et al. (2022) reviewed the evolution of ankle–foot orthoses with emphasis on material selection, actuation mechanisms, and biomechanical performance, providing valuable insights for future orthotic design. Gupta et al. (2023) comprehensively reviewed current and emerging ankle and foot arthroplasty and prosthetic systems, discussing advancements in materials, fixation strategies, and long-term clinical outcomes. Chen et al. (2023) summarized clinically relevant finite element models

of the natural ankle joint, emphasizing modeling techniques used to predict stress, strain, and joint stability under physiological loading. Lewis et al. (2025) investigated the influence of keel geometry on total ankle prosthesis biomechanics and demonstrated that keel shape significantly affects stress transfer and implant durability. Wang et al. (2024) analyzed the biomechanical effects of novel polyethylene insert configurations in ankle prostheses and reported reduced interface stress and micromotion with optimized designs. Petrović et al. (2023) performed a dynamic finite element comparison of customized total talar replacement and total ankle replacement, revealing distinct differences in load transfer and joint stability during gait. Rasheed and Kahtan (2024) proposed an improved prosthesis for through-ankle amputation and validated its performance using finite element analysis, showing reduced stress concentration and improved structural safety. Collins et al. (2025) developed a motorized compliant ankle prosthesis (RoboANKLE) to replicate natural ankle torque profiles, with simulation results indicating enhanced biomechanical performance during walking. Additionally, Liu et al. (2023) proposed a flexible bionic ankle prosthesis using subject-specific modeling techniques, which improved user comfort and minimized abnormal stress on the residual limb.

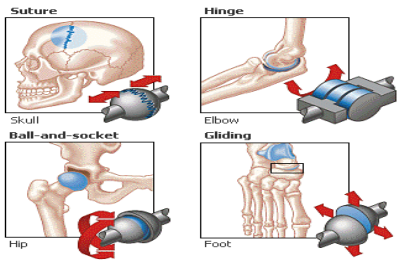

Figure 1 Various joints in a human body

1.2 Parts of a joint

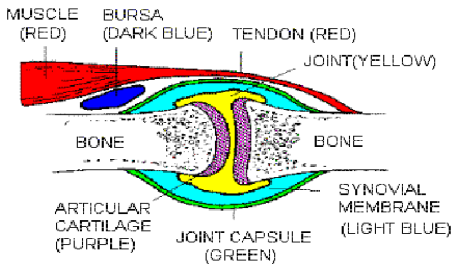

Figure 2 Parts of a joint

1.3 ANATOMY OF LOWER EXTREMITY

Femur

The femur, commonly known as the thigh bone, is the longest and most robust bone in the human skeleton, extending from the hip to the knee. As the primary structural support for the body's weight, it is exceptionally strong, providing the stability and leverage necessary for the movement of the lower limbs.

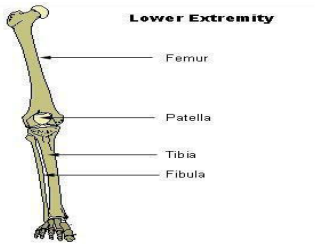

Figure 3 Anatomy of Lower Extremity

1.4 ANATOMY OF THE FOOT

The human foot is structured into three distinct anatomical planes and three primary bone segments that facilitate complex movement. The frontal, transverse, and sagittal planes provide the lower leg with three degrees of freedom, allowing for a wide range of motion and rotation. Structurally, the foot is categorized into the hindfoot, midfoot, and forefoot,

each serving a specific role in stability and locomotion.

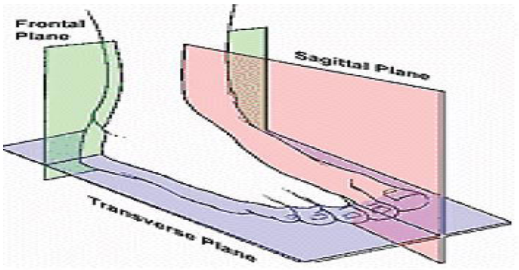

Figure 4 Anatomical planes of the foot and ankle (frontal, transverse and sagittal)

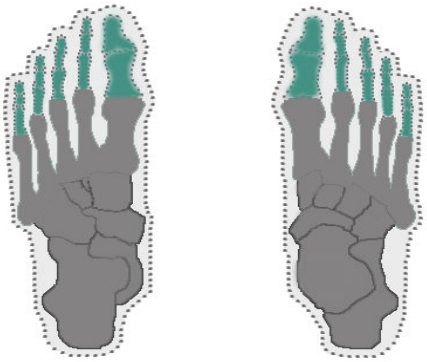

Figure 5 LIST OF ALL DIGITS OF THE FEET (TOE BONES OR PHALANGES)

proximal phalanges (5 × 2), intermediate phalanges (4 × 2), distal phalanges (5 × 2)

Distal Phalanges

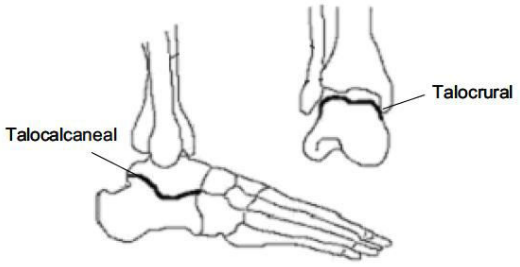

Figure 6 Major two ankle joints talocalcaneal joint and talocrural joint

. in the

(A) lateral view and the (B) posterior view [6].

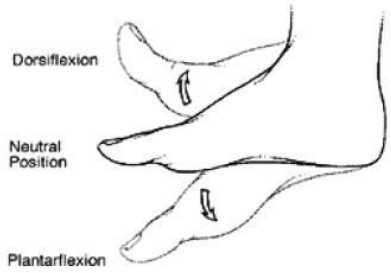

Figure 7 Sagittal plane movement- dorsiflexion and plantar flexiona

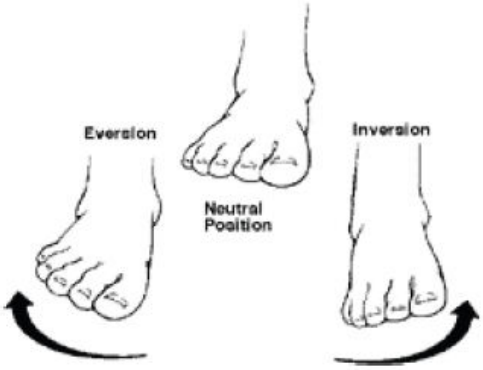

Figure 8 Frontal plane movement- eversion and inversiona

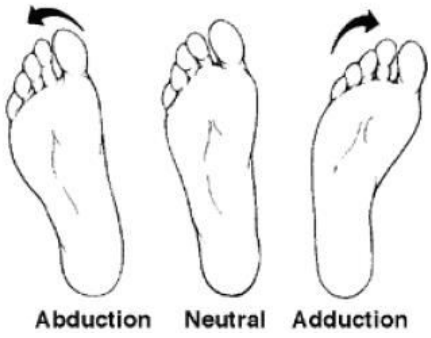

Figure 9 Transverse plane movement . abduction and adductiona

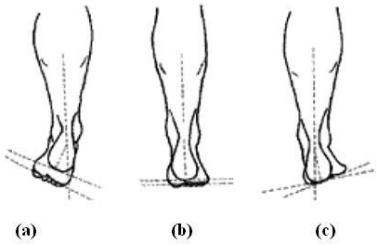

Figure 10 Tri-planar movement of the ankle

. (A) supination, (B) Neutral and

(C) pronationa

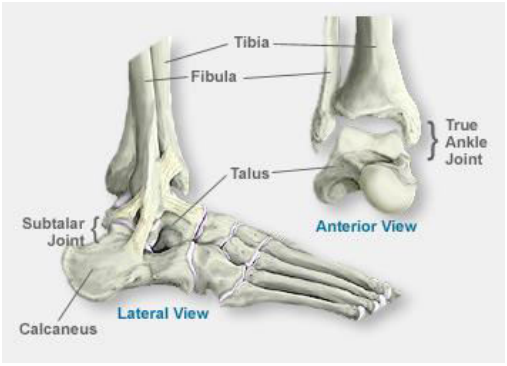

Figure 11 Anterior and Lateral view of the ankle2

TOTAL ANKLE REPLACEMENT

Ankle replacement, also known as ankle arthroplasty, is a surgical procedure designed to replace the damaged articular surfaces of the ankle joint with prosthetic components. This method is increasingly becoming the preferred treatment for patients, often replacing the traditional use of arthrodesis, or joint fusion. The primary advantage of ankle replacement over fusion is its ability to restore a natural range of motion, which is critical for maintaining fluid movement and overall joint function.

LITERATURE REVIEW

Recent research on ankle joints, ankle prostheses, and total ankle replacement (TAR) has focused on improving biomechanical performance, functional mobility, durability, and patient-specific customization through advanced materials, intelligent control, and simulation-based design.

H. M. Nazha et al. (2024) investigated material performance in artificial ankle joints using biomechanical analysis. Their study compared commonly used implant materials under physiological loading conditions and highlighted the importance of wear resistance, strength, and compatibility in extending implant lifespan. The findings emphasize that appropriate material selection significantly influences joint stability and long-term clinical success.

S. Akhmejanov et al. (2025) designed an autonomous active ankle–foot prosthesis with two degrees of freedom to better replicate natural ankle motion. Using sensors and control systems, the device demonstrated improved adaptability during walking on uneven terrain. This work shows the growing shift toward powered prostheses that restore dynamic gait rather than merely providing passive support.

J. M. Lee and S. W. Lee (2025) proposed a novel method for determining component size in total ankle replacement. Their approach reduces implant mismatch by considering anatomical variations, which is critical for minimizing postoperative complications and improving functional outcomes. Accurate sizing was shown to enhance load distribution and joint alignment.

M. Hassan et al. (2026) modeled a porous mobility total ankle arthroplasty implant using computational simulations. The porous structure was designed to promote bone ingrowth while maintaining mechanical strength. Results indicated improved stress distribution and reduced risk of implant loosening, suggesting that porous designs can enhance long-term fixation.

B. Li et al. (2024) developed an intelligent ankle–foot prosthesis inspired by human anatomical structure and motion bionics. Incorporating motion sensors and adaptive control algorithms, the prosthesis was able to mimic natural ankle behavior during different phases of gait, thereby improving user comfort and mobility.

A. Pace, J. Gardiner, and D. Howard (2025) presented a simulation-based design of a cam-driven hydraulic prosthetic ankle. Their design produced smoother motion and more natural torque generation compared with conventional passive devices. Hydraulic

mechanisms were shown to effectively absorb shock and assist push-off during walking.

C. Zhou et al. (2022) provided a comprehensive review of ankle–foot orthoses (AFOs), discussing their evolution, design principles, materials, and clinical applications. The study highlighted the role of AFOs in rehabilitation for neurological and musculoskeletal disorders and emphasized the trend toward lightweight, energy-storing designs.

R. Gupta et al. (2023) reviewed current and future designs of ankle and foot arthroplasty and prostheses. The authors discussed advances in biomaterials, fixation methods, and joint mechanics, noting that modern designs aim to restore natural kinematics while reducing wear and loosening. Emerging technologies such as additive manufacturing and smart implants were identified as promising directions.

S. Chen et al. (2023) reviewed clinically useful finite element (FE) models of the natural ankle joint. Their work demonstrated that FE analysis is a powerful tool for predicting stress distribution, ligament behavior, and implant performance. Accurate modeling was found essential for optimizing prosthesis design before clinical implementation.

J. F. Lewis et al. (2025) examined the influence of keel shape on total ankle prosthesis biomechanics. Different keel geometries were shown to significantly affect implant stability and stress transfer to surrounding bone. Optimized keel design can reduce the risk of loosening and improve fixation strength.

L. Wang et al. (2024) studied the effect of polyethylene insert configuration on ankle prosthesis biomechanics. Their results indicated that insert geometry influences contact pressure, wear characteristics, and joint mobility. Proper configuration is therefore crucial for balancing stability and range of motion.

A. Petrović et al. (2023) conducted dynamic finite element analysis comparing customized total talar replacement with total ankle replacement. Customized talar implants showed favorable stress distribution and functional performance, suggesting that patient-specific solutions may outperform standard implants in certain cases.

N. K. Rasheed and Y. Y. Kahtan (2024) developed an improved prosthesis for through-ankle amputation. Their design focused on enhancing comfort, stability, and weight distribution, addressing common issues faced by amputees using traditional devices.

M. Collins et al. (2025) introduced RoboANKLE, a motorized compliant ankle prosthesis designed to produce natural torque profiles during walking. By combining motor actuation with compliant elements, the device improved energy efficiency and gait symmetry, representing progress toward fully powered, biomimetic prostheses.

Y. Liu et al. (2023) designed a flexible bionic ankle prosthesis using subject-specific modeling. Customization based on individual anatomy allowed better alignment, improved motion, and reduced discomfort, highlighting the importance of personalized prosthetic solutions.

2.1 HISTORY OF TOTAL ANKLE REPLACEMENT (TAR)

The origins of total ankle arthroplasty can be traced to the 1970s, a period marked by the increasing success and popularity of total hip and knee replacements. During this era, engineers and surgeons initially viewed the development of an ankle prosthesis as a relatively simple endeavor, resulting in the creation of various early designs. However, these first-generation models were generally characterized by cemented, two-part configurations that failed to accurately replicate the natural anatomy of the human joint.

2.2 NEED FOR TOTAL ANKLE REPLACEMENT (TAR)

Because the ankle is a primary weight-bearing joint that supports the body's entire mass, managing chronic pain in this area is essential for mobility. Severe ankle pain can be debilitating, often making surgical intervention like ankle replacement a necessary solution. As an alternative to joint fusion (arthrodesis) for select patients, ankle replacement serves as an effective option for pain relief. It is

typically pursued only after conservative treatments—such as physical therapy or medication—have failed to alleviate persistent discomfort or correct joint deformities.

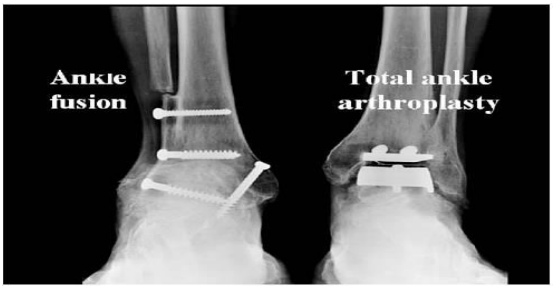

Figure 12 Right ankle arthrodesis and left ankle arthroplasty performed sequentially

2.3 CURRENT IMPLANTS AND FAILURES

In 2005, the total volume of ankle replacement procedures, including revisions, reached approximately 7,000 cases. With a projected annual growth rate of 6% to 8%, this figure was estimated to rise to 11,000 procedures by 2012. Mirroring this clinical expansion, the industry-wide revenue generated by these surgeries was expected to climb from $285 million to $476 million over the same period.

2.3.2 The Scandinavian Total Ankle Replacement (STAR)

The **Surgical Total Ankle Replacement (STAR)** is one of the most widely utilized prostheses for ankle arthroplasty. It is categorized as a non-constrained total ankle replacement, designed to surgically restore the function of a damaged joint. The "non-constrained" nature of the STAR ankle is a key feature, as it allows the bearing to move freely across multiple planes along the tibial component, more closely mimicking the natural biomechanics of the human ankle.

Figure 13 STAR ankle

2.4 MATERIAL PROPERTIES

MATERIAL PROPERTIES	COCRMO	TI-6AL-7NB	TI-13Nb-13-Zr	SS STAINLESS STEEL 316L
Density(g/cm³)	1.25	4520	4510	7850
Possion's Ratio	0.38	0.33	0.33	0.30
Young's Modulus(Gpa)	2.5	105-110	75-85	200-210
Ultimate Tensile Strength (Mpa)	29.6	880-920	900-1030	400-450

Table 1 MATERIAL PROPERTIES

3 DESIGN OF AN ARTIFICIAL ANKLE JOINT IN CATIA V5 R20

CATIA, which stands for **Computer Aided Three-dimensional Interactive Application**, is a comprehensive multi-platform software suite for CAD, CAM, and CAE. Developed by the French company **Dassault Systèmes** and supported globally by IBM, it is recognized as the world's most powerful and widely utilized knowledge-based design software. Due to its advanced capabilities, it is the industry standard across a vast range of sectors, including aerospace, automotive, shipbuilding, architecture, and medical device manufacturing.

Material Used – COCRMO, TI-6AL4V, SS L 316, TI-6AL-7NB

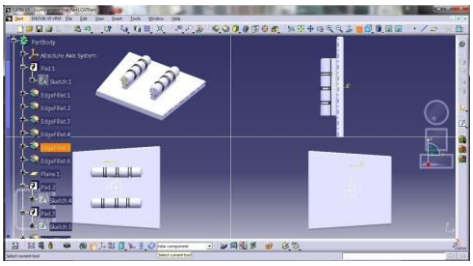

Figure 14 Design of tibial component

3.1 Design of mobile bearing component

SPECIFICATIONS OF A BEARING COMPONENT

Length of bearing component = 30mm

Width of bearing component = 20mm

Height of bearing component = 8mm

Material used- COCRMO, TI-6AL4V, SS L 316, TI-6AL-7NB

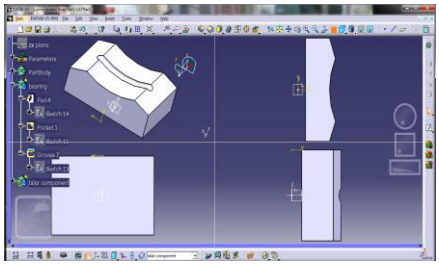

Figure 15 Design of mobile bearing component

3.2 Design of talar component

SPECIFICATIONS OF TALAR COMPONENT

The elements of talar segment were taken.

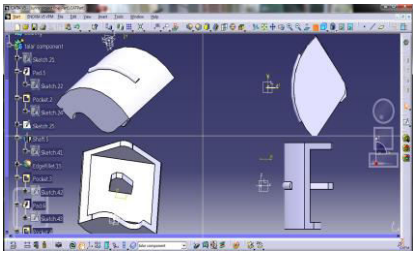

Figure 16 Design of mobile bearing component

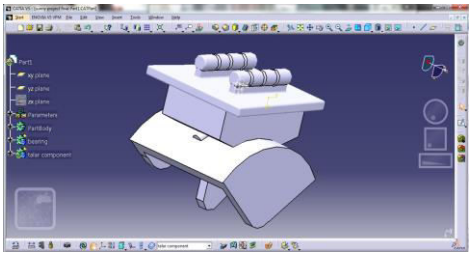

Figure 17 Design of an artificial ankle joint

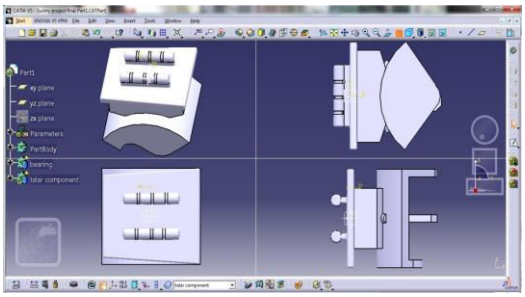

Figure 18 Different views of artificial ankle joint

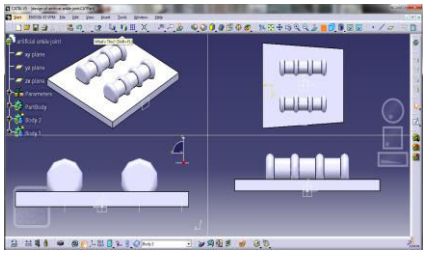

Figure 19 Design of tibial component similar to STAR tibial component

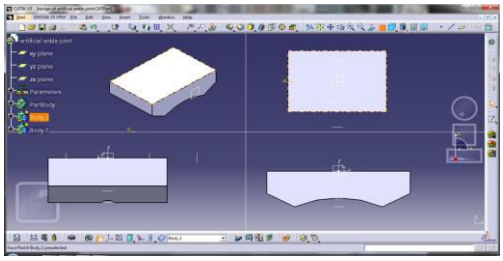

Figure 20 Design of bearing component similar to STAR bearing component

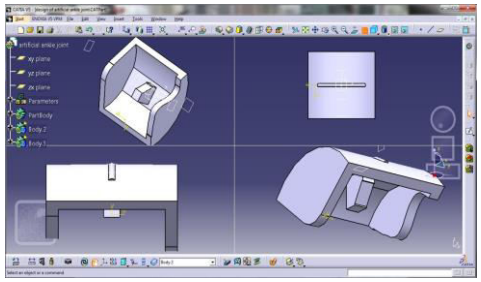

Figure 21 Design of talar component similar to STAR talar component

4 NON-LINEAR STATIC ANALYSIS OF AN ARTIFICIAL ANKLE JOINT

4.1 MESHING :

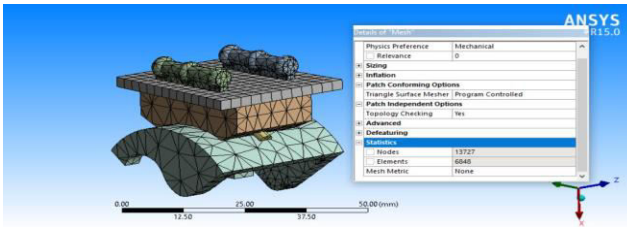

Figure 22 Meshing Nodes: 13727, Elements: 6848.

4.2 BOUNDARY CONDITIONS:

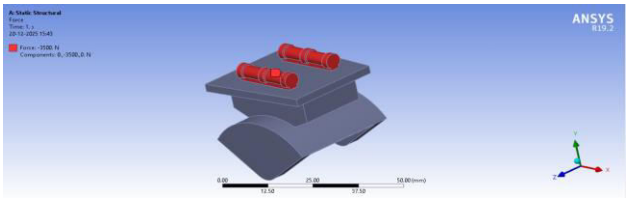

Figure 23 Boundary condition Load 3500N

5 RESULTS AND DISCUSSIONS

5.1 STATIC ANALYSIS AT 2500N:

CoCrMo Material:

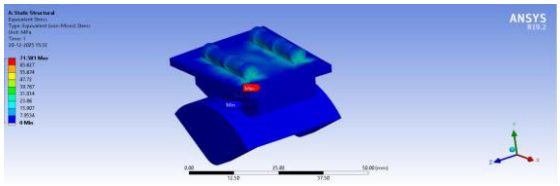

Figure 24 Von-misses stresss of CoCrMo Material at 2500N

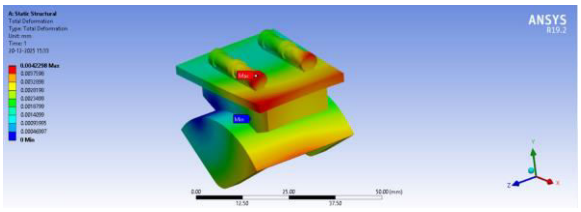

Figure 25 Total deformation of CoCrMo Material at 2500N

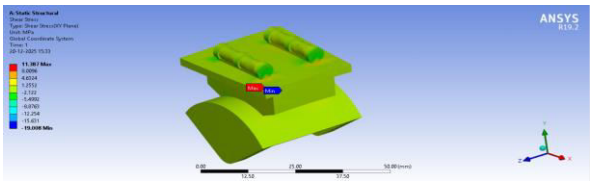

Figure 26 Shear stress of CoCrMo Material at 2500N

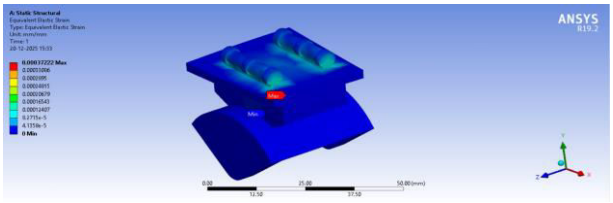

Figure 27 Strain of CoCrMo Material at 2500N

Ti-6Al-7Nb Material:

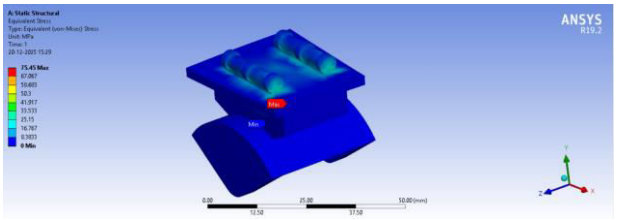

Figure 28 Von-misses stress of Ti-6Al-7Nb Material at 2500N

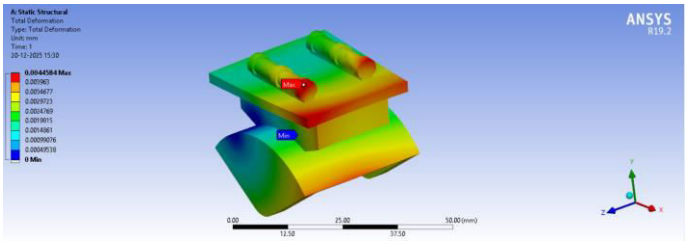

Figure 29 Total deformation of Ti-6Al-7Nb Material at 2500N

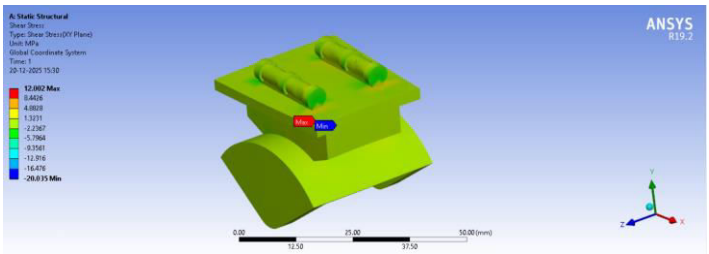

Figure 30 Shear stress of Ti-6Al-7Nb Material at 2500N

6.1 ANATOMY OF A 3D PRINTER:

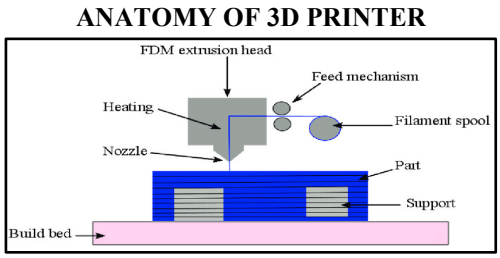

Figure 32 FUSED DEPOSITION MODELING

Figure 33 Ankle Joint Bottom View

The obtained model is exported in STL file format which can be later used for other applications.

6.2 CODING OF 3D PRINTING

PROCESS OF 3D PRINTING
;FLAVOR: Marlin
; TIME:8085
;Filament used: 4.62471m
;Layer height: 0.2
;MINX:91.456
;MINY:93.45
;MINZ:0.2
;MAXX:137.595
;MAXY:141.55
;MAXZ:35

6.3 GRAPHS:

6.3.1 VON-MISSES STRESS GRAPH:

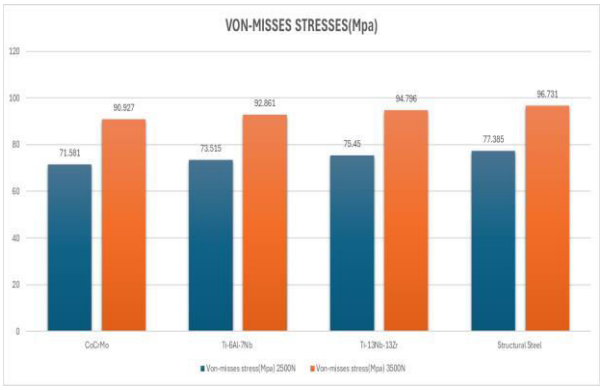

Graph 1 Von-misses stress graph

6.3.2 TOTAL DEFORMATION GRAPH:

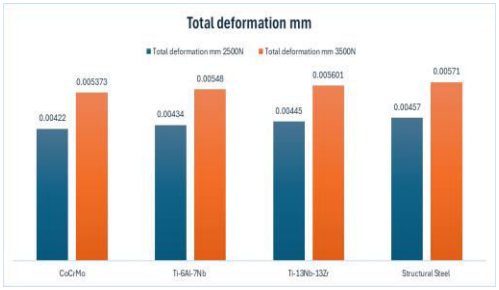

Graph 2 Total Deformation Graph

6.3.3 SHEAR STRESS GRAPH:

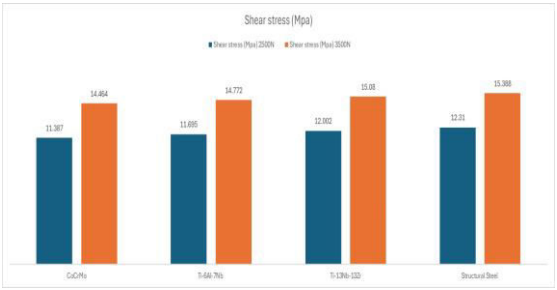

Graph 3 Shear Stress Graph

6.3.4 STRAIN:

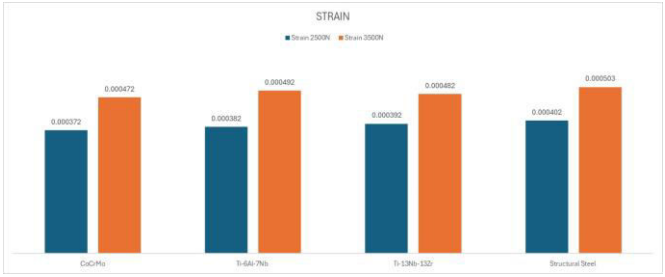

Graph 4 Strain

6.5 MODAL ANALYSIS:

COCRMO Materials	Total deformation(mm)	Frequency(Hz)
Mode 1	3.642	0.024
Mode 2	6.423	1.613
Mode 3	7.164	10.432

7 CONCLUSIONS

The design and structural analysis of the ankle joint were successfully executed using **CATIA** and **ANSYS**, focusing on static and modal behaviors under physiological loads of 2500 N and 3500 N. The study revealed a linear correlation between load and stress across all materials; however, **Cobalt-Chromium-Molybdenum (CoCrMo)** consistently emerged as the superior material for implants. It exhibited the lowest von Mises stress (71.581 MPa to 90.927 MPa) and shear stress (41.328 MPa to 52.483 MPa), alongside the highest natural frequencies and minimal deformation (0.161 mm). While titanium alloys like **Ti-6Al-7Nb** and **Ti-13Nb-13Zr** offered moderate performance, **SS 316** demonstrated significantly lower stability with a high deformation of 3.642 mm. Ultimately, the exceptional stiffness and vibration resistance of CoCrMo make it the most suitable choice for ensuring long-term durability and safety under the extreme biomechanical pressures of human movement.

FUTURE SCOPE

1.FATIGUE AND WEAR ANALYSIS

Future research should expand upon this study by incorporating long-term fatigue, wear, and contact stress analyses of **CoCrMo** ankle joint implants. By subjecting the prosthetic components to cyclic loading, researchers can more accurately simulate real-life gait cycles and various daily physical activities. This longitudinal approach is essential for predicting the mechanical endurance of the implant and understanding how repeated stress impacts the structural integrity and surface wear of the material over time.

2.BIO-TRIBOLOGICAL AND CLINICAL EVALUATION

To achieve clinical validation, future research should investigate the wear debris behavior, corrosion resistance, and biocompatibility of **CoCrMo** in direct comparison with advanced titanium alloys. By conducting both **in-vitro** (laboratory-controlled) and **in-vivo** (living organism) studies, researchers can assess how these materials interact with the biological environment over time. This comparative analysis is vital for identifying potential inflammatory responses to metallic particles and ensuring that the chosen alloy maintains its chemical stability when exposed to bodily fluids.

3.DESIGN OPTIMIZATION AND PATIENT-SPECIFIC IMPLANTS

Future advancements in prosthetic design should focus on developing optimized, patient-specific ankle implant geometries through the integration of **topology optimization** and **additive manufacturing**. By utilizing computational algorithms to refine the implant's shape, engineers can strategically redistribute material to minimize stress concentrations and better mimic individual patient anatomy. Furthermore, the use of 3D printing (additive manufacturing) allows for the creation of complex, porous structures that promote better bone ingrowth, ultimately enhancing the longevity, comfort, and overall success rate of the implant.

REFERENCES

- H. M. Nazha et al., “Investigating material performance in artificial ankle joints: A biomechanical study,” *Prosthesis*, vol. 6, no. 3, Article 36, 2024.
- S. Akhmejanov et al., “Design and analysis of an autonomous active ankle–foot prosthesis with two degrees of freedom,” *Sensors*, vol. 25, no. 16, Article 4881, 2025.
- J. M. Lee and S. W. Lee, “A novel approach to determine component size in total ankle replacement,” *Scientific Reports*, vol. 15, Article 13004, 2025.

∟ M. Hassan et al., “Modeling and simulation of a porous mobility total ankle arthroplasty implant,” *Journal of Orthopaedic Surgery and Research*, vol. 20, no. 1, Article 601, 2026.

∟ B. Li et al., “Intelligent ankle–foot prosthesis based on human structure and motion bionics,” *Journal of NeuroEngineering and Rehabilitation*, vol. 21, no. 1, Article 114, 2024.

∟ A. Pace, J. Gardiner, and D. Howard, “Simulation-based design of a cam-driven hydraulic prosthetic ankle,” *Prosthesis*, vol. 7, no. 1, Article 9, 2025.

∟ C. Zhou et al., “Research and development of ankle–foot orthoses: A review,” *Sensors*, vol. 22, no. 14, Article 5384, 2022.

∟ R. Gupta et al., “Ankle and foot arthroplasty and prosthesis: Current and future designs,” *Micromachines*, vol. 14, no. 11, Article 2081, 2023.

∟ S. Chen et al., “Clinically useful finite element models of the natural ankle joint: A review,” *Clinical Biomechanics*, vol. 104, Article 105901, 2023.

∟ J. F. Lewis et al., “Influence of keel shape on total ankle prosthesis biomechanics,” *Journal of Foot and Ankle Surgery*, vol. 64, no. 2, pp. 289–297, 2025.

∟ L. Wang et al., “Effect of polyethylene insert configuration on ankle prosthesis biomechanics,” *Frontiers in Bioengineering and Biotechnology*, vol. 12, Article 1371851, 2024.

∟ A. Petrović et al., “Dynamic finite element analysis comparing customized total talar replacement and total ankle replacement,” *Journal of Orthopaedic Surgery*, vol. 31, no. 3, 2023.

∟ N. K. Rasheed and Y. Y. Kahtan, “An improved prosthesis for through-ankle amputation,” *Al-Khwarizmi Engineering Journal*, vol. 20, no. 2, pp. 45–56, 2024.

∟ M. Collins et al., “RoboANKLE: A motorized compliant ankle prosthesis for natural torque profiles,” *arXiv preprint*, arXiv:2510.14414, 2025.

∟ Y. Liu et al., “Design of a flexible bionic ankle prosthesis with subject-specific modeling,” *Journal of Bionic Engineering*, vol. 20, no. 4, pp. 1021–1034, 2023.